Curvature from multipartite entanglement in quantum gravity states

Simone Cepollaro[*]
Scuola Superiore Meridionale, Largo S. Marcellino 10, 80138 Napoli, Italy and INFN–Sezione di Napoli, Via Cinthia, 80126, Napoli, Italy

Goffredo Chirco,[†] Gianluca Cuffaro,[‡] and Vittorio D'Esposito[§]
Dipartimento di Fisica "Ettore Pancini," Università di Napoli Federico II, Napoli, Italy and INFN–Sezione di Napoli, Via Cinthia, 80126, Napoli, Italy

(Received 8 May 2023; accepted 26 July 2023; published 16 August 2023)

We investigate multipartite entanglement in quantum geometry states described by loop quantum gravity spin networks. We focus on states corresponding to *bounded* regions of 3D spacelike slices of spacetime with nonvanishing intrinsic curvature, realized via spin networks defined on a graph with nontrivial $SU(2)$ holonomies. The presence of intrinsic curvature in the region is encoded—via coarse graining—into *tag* spins attached to the vertices of the graph. The resulting states are generalized bulk-to-boundary maps defined in an *extended* boundary Hilbert space comprised by the spin representations carried by the tags and by the uncontracted edges at the boundary. We consider a *tripartition* of a *random* quantum geometry state in the extended-boundary space consisting of a bipartite boundary subsystem and a bulk-tags complement, and we propose a measure of logarithmic negativity to study the change in the entanglement phases of the boundary marginal mixed state, while varying the dimension of the bulk curvature environment. In the large spin regime, we find that the *typical* entanglement negativity is well described by the *generalized Page curve* of a tripartite random state. In particular, we find area scaling behavior of negativity for small curvature, while for large curvature the negativity vanishes, suggesting an effective thermalization of the boundary. Remarkably, the positive partial transpose character of the mixed boundary state corresponds to a change in the effective topology of the network, with the two boundary subregions becoming disconnected.

DOI: 10.1103/PhysRevD.108.046010

I. INTRODUCTION

In the last two decades, the idea of a correspondence between geometry and entanglement, suggesting quantum correlations as the fabric of an emergent continuum, classical spacetime, has radically changed all approaches to quantum gravity [1–9]. Beside the AdS/CFT framework [10], where an entanglement-geometry correspondence is reflective of the gauge/gravity duality [11–15], nonperturbative and background-independent approaches to quantum gravity recently offered a new playground to investigate the roots of such an interplay.

In loop quantum gravity [16–18], and related generalizations like spinfoams theory and group field theory [19,20], a beautiful quantization of space at one time is realized in terms of superpositions of *quantum spin networks* [21–23]. These are $SU(2)$ gauge symmetric tensor networks, defined by *graphs* with edges labeled by $SU(2)$ spin *irreps* and vertices dressed by intertwining operators, which encode geometric and topological features of $3D$ geometry into purely algebraic and combinatorial degrees of freedom [18]. Quantum geometry states described in terms of spin networks as functionals of the $SU(2)$ Ashtekar-Barbero connections essentially capture the *kinematics* of general relativity in its first order formulation [24], which can be eventually described in analogy with the conventional Hilbert space of an $SU(2)$ lattice Yang-Mills theory [25,26]. This makes spin networks a phenomenal quantitative tool to investigate the operational content of the gravitational field, reduced on $3D$ spacetime slices, at the quantum scale [27–38].

In this light, spin-network entanglement has become a central resource to characterize physical vacuum states of the theory [39–42], investigating *local* holographic

[*]simone.cepollaro-ssm@unina.it
[†]goffredo.chirco@unina.it
[‡]g.cuffaro@studenti.unina.it
[§]vittorio.desposito@unina.it

properties of quantum spacetime geometry [43–45] and ultimately to study the emergence of classical spacetime geometry with its classical symmetries from its quantum description, with a renovate interplay of techniques and tools from quantum information theory, information geometry, quantum many-body theory, and quantum computation theory more recently [46–57].

Much work in the field has recently focused on quantum $3D$ geometry states with $2D$ boundaries, corresponding classically to spacetime spatial slices with *corners* [58], thereby looking at quantum spin networks with boundaries as *boundary maps* with corner states encoding the geometric and topological information stored in the bulk correlation structure. In this setting, different measures of multipartite entanglement have been proposed to investigate encoding and decoding of bulk information in the boundary/bulk mapping [59–61] and its holographic behavior.

In [35,62–66], the holographic character of the spin networks' boundary/bulk mapping has been investigated within a quantum typical regime starting from a *random* tensor-network description of $3D$ quantum geometry states in the large spin limit [9,67,68]. Along this line, inspired by recent work in [69–72], in [61] the measure of *entanglement negativity* was first proposed to extend the study of the hierarchy of boundary correlations to *multipartite* quantum spin-network states, beyond the bipartite pure-state setting of entanglement entropy.

In this work, we consider a description of a uniformly curved quantum $3D$ space region with boundary realized in terms of a *tagged* open spin-network state in loop quantum gravity [73,74]. We show that the effective topology of this region is reflected in the multipartite entanglement of the state. In the presence of curvature in the region, we generalize the bulk-to-boundary mapping description of the open spin network [59–61] as to include the space of bulk defects in an *extended boundary* state ρ_τ, where bulk information is *shared* among entangled boundary spins and tags: surface and intrinsic curvature of the quantum space region are entangled.

We consider a tripartition of the extended boundary system into three subsystems A_1, A_2, B, with A_1, A_2 complementary regions of the external boundary, and B the set of tags in the bulk. This corresponds to a factorization of the extended boundary Hilbert space, for fixed tags and boundary edges spins. We model the $2D$ corner quantum geometry state on the reduced density matrix obtained by tracing over the tags spins in B, and we evaluate the entanglement of the resulting mixed state $\rho_{A_1A_2} = \mathrm{Tr}_B[\rho_\tau]$ by computing the *logarithmic negativity* of its *partial transpose* [28,61,69,72,75]. Indeed, the Peres criterion [76] guarantees that the presence of *negative* eigenvalues in the partial transpose $\rho^{T_{A_2}}_{A_1A_2}$ *witnesses* quantum correlations in $\rho_{A_1A_2}$ [77].

We find that the quantum correlations of the boundary state include both intertwiner entanglement as well as correlations among bulk and boundary edges and tags spins. We focus our analysis on the latter contributions.

In the typical regime, corresponding to a large spin (semiclassical) limit for our system, we show that the degree of quantum correlations among boundary subregions depends on the dimension of the bulk tags system, which plays the role of a hidden environment from the viewpoint of a generic observer measuring correlations on the boundary. As an effect of the *monogamy* of entanglement, when the bulk curvature environment is much smaller than the boundary system, the entanglement negativity of the boundary subregions displays the area law behavior of a bipartite random pure state. However, when the environment dominates, the negativity vanishes suggesting an effective thermalization of the boundary, with the boundary subregions becoming effectively disconnected. In an intermediate regime, peculiar to the tripartite setting, the curvature environment mediates the entanglement of the boundary. In this case, the logarithmic negativity E_N scales with the area of the cluster boundary with a negative correction which depends linearly on the number of tags. As derived in detail in Sec. VII B, we find in this regime a generalization of the Ryu-Takayanagi formula for entanglement entropy for the tripartite setting, in agreement with [61,69], which can trace back logarithmic negativity to a *mutual information* between the subsystem A_1 and A_2. All these three regimes can be easily achieved by only tuning one *entanglement phase parameter* q, which is actually the ratio between the number of tags (bulk curvature inside the curved region) and the number of boundary spins (total area bounding the curved region).

Moreover, in the loop quantum gravity setting, we find that the geometric characterization of our networks' states relates the entanglement negativity, expressed in terms of areas of the bounded $3D$ region, to the intrinsic scalar curvature of the region. Indeed, as better clarified in Sec. VIII, under some reasonable semiclassical assumptions about areas of curved surfaces we are able to relate in a nice way our entanglement phase parameter q to the *Ricci curvature* of a given 3D spacetime slice for any coarse-graining scale ε. We find in particular that $q \propto \mathcal{R}\varepsilon^2$, with $\mathcal{R}$ being the Ricci curvature. Such a behavior suggests a possible role of the multipartite description of quantum geometry in modeling quantum spacetime curvature and singularities in quantum gravity.

The paper is organized as follows. Section II introduces loop quantum gravity quantum geometry states as superpositions of quantum spin networks. In Sec. III, this notion is generalized to include boundaries and nontrivial topology. In particular, here we define quantum states associated with regions of bounded $3D$ space with nonvanishing intrinsic curvature. Section IV introduces the

notion of tagged spin networks, which is the starting point of our characterization of the bounded quantum geometry as a mixed state. In Sec. V, we define the tripartition $\{A_1, A_2, B\}$ of our system, with A_1, A_2 corresponding to complementary subregions of the boundary and B referring to the set of *tags* produced by the integral (partial tracing) over the nontrivial loop holonomies in the bulk. For such a tripartite system, we quantify the entanglement of the boundary via a measure of *typical* entanglement negativity [76–82] by considering the boundary mapping on a bulk state *prepared at random*. The random measurement combined with the boundary map projection allows us to limit the partial tracing to the "curvature" degrees of freedom, while (partially) retaining the information on the graph structure. We compute typical kth order Rényi log-negativity for even k via replicas by mapping momenta of the A_1, A_2 reduced density matrix to partition functions of a classical generalized Ising model [69,72], hence looking for the minimal free energy configurations of the model. In Sec. VI, we characterize the bulk state contributions to the free energy of the classical model. The analysis is thereby restricted to states with small intertwiner entanglement. Section VII contains an explicit example of an open spin-network state—a cluster of tags—with four vertices. For such a simplified setting, we can explicitly compute the typical logarithmic negativity of the mixed boundary state in the large spin regime and characterize the entanglement phase diagram of the boundary state. This section contains the main results of the paper. Finally, we close in Sec. VIII with a summary of the results and some closing remarks.

II. SPIN NETWORKS STATES

Loop quantum gravity (LQG) space of 3D geometry is realized as a space of square-integrable functions,

$$H_\gamma = L^2[SU(2)^{\times E}/SU(2)^{\times V}], \tag{1}$$

with support on closed oriented graphs γ comprised by V vertices connected by E edges. States in H_γ depend on one group element $g_e \in SU(2)$ for each edge e of the graph and are assumed to be invariant under the $SU(2)$ action at each vertex v, that is, $\forall\ h \in SU(2)$,

$$\begin{aligned}\psi_\gamma &: SU(2)^{\times E} \to \mathbb{C}\\ &\{g_e\}_{e\in\gamma} \mapsto \psi_\gamma(\{g_e\}) = \psi_\gamma(\{h_{t(e)} g_e h_{s(e)^{-1}}\}),\end{aligned} \tag{2}$$

where $t(e)$ and $s(e)$ respectively refer to the target and source vertices of the edge e [83]. In the geometrical interpretation of loop quantum gravity, spin network vertices are dual to $3D$ atoms of space described by quantized convex polyhedra, with a number of faces given by the valence of the vertex. Edges attached to the vertices are dual to faces of the polyhedron [84]. In this light, intertwiners' quantum numbers represent $3D$ volume excitations while the values of the edge spins represent 2D area excitations. Polyhedra corresponding to adjacent vertices are glued together via their faces. By construction, the area of two glued faces match, while their shapes do not have to. In this sense, spin-network states living in H_γ have a natural geometrical interpretation in terms of discrete (twisted) geometries [85].

For $SU(2)$ as a compact Lie group, by the Peter–Weyl theorem, functions of d group elements g can be decomposed into irreducible representations (irreps) of the group,

$$f(\{g\}) = \sum_{\{j\}} \sum_{\{m\}\{n\}} f^{\{j\}}_{\{m\}\{n\}} \prod_{i=1}^{d} d_{j_i} D^{j_i}_{m_i n_i}(g_i), \tag{3}$$

with $\{j_i\} \in \mathbb{N}/2$ labeling irreducible representations (irreps) of $SU(2)$; indices m_i (n_i) labeling a basis in the vector space $V^{j_i} = \mathrm{span}\{|j_i, m_i\rangle\}$, carrying the representation j_i, of dimension $d_{j_i} = 2j_i + 1$, and $D^{j_i}_{m_i n_i}(g_i) = \langle j_i, n_i | g_i | j_i, m_i\rangle$ the Wigner matrix representing the group element g_i.

This allows us to write $SU(2)$-invariant functions ψ_γ as *superpositions* of gauge symmetric tensor networks with fixed spins $\{j\}_\gamma$ and the connectivity of the graph γ. Two vertices of the graph, say v and w, are connected by edge states labeled by a spin j irrep of $SU(2)$ and dressed with a group element $g_e \in SU(2)$, that is,

$$|e_{vw}(g_e)\rangle \equiv \sum_{\{m\}\{n\}} \frac{(-1)^{j-n}}{\sqrt{d_j}} D^j_{mn}(g_e) |j, m\rangle_v \otimes \overline{|j, n\rangle}_w \tag{4}$$

in the Hilbert space $H_{vw} = [V^j_v \otimes \bar{V}^j_w]$. At each vertex v of the graph, an intertwiner operator ι_v enforces $SU(2)$ gauge invariance via a projection

$$\iota_v : \bigotimes_{e\in v} V_{j_e} \to V_0, \tag{5}$$

corresponding to a recoupling of the edges spins at the vertex in the $SU(2)$-symmetric (singlet) representation with $j = 0$. This associates to each vertex the degeneracy space of V_0 for fixed $\{j_e\}$,

$$H_v = \mathrm{Inv}_{SU(2)}\left[\bigotimes_{e\in v} V^{j_e}\right] = \mathrm{span}\{|\iota_v\rangle\}, \tag{6}$$

with $|\iota_v\rangle$ an orthonormal basis in H_v.

A *spin network* state $|\gamma, \{j_e\}, \{\iota_v\}\rangle$ is thereby defined as the assignment of representation labels $\{j_e\}$ to each edge of γ and the choice of a vector $|\{\iota_v\}\rangle$ in $H_V = \bigotimes_v^V H_v$ for the vertices, corresponding to the contraction (see Fig. 1)

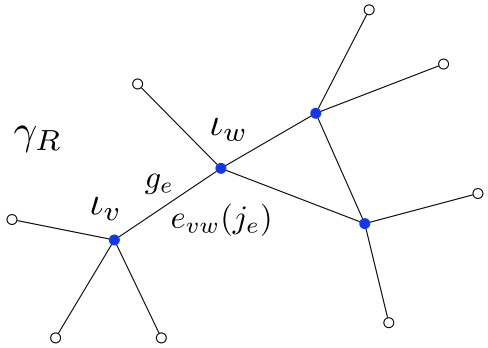

FIG. 1. Open spin network with support on the graph γ_R. The boundary is comprised of the set of not contracted edges with dangling magnetic indices pictured as empty circles.

$$\langle\{g_e\}|\gamma,\{j_e\},\{i_v\}\rangle = \left(\bigotimes_{e=1}^{E}\langle e(g_e)|\right)|\{\iota_v\}\rangle. \tag{7}$$

Such spin networks define an orthogonal basis in H_γ, for the following isomorphism holds:

$$H_\gamma \approx \bigoplus_{\{j\}} H_V. \tag{8}$$

In particular, we will write the quantum $3D$ geometry state $|\psi_\gamma\rangle$ as the *contraction* of a generic collective intertwiner state $|\psi\rangle$ in H_V with the set of E edge states comprising the graph, via a sum over spins

$$|\psi_\gamma(\{g_e\})\rangle = \sum_{\{j_e\}}\left(\bigotimes_{e=1}^{E}\langle e(g_e)|\right)|\psi\rangle, \tag{9}$$

where the contraction amounts to a sum over bulk indices. In the expression above, the sum over the intertwiner index is included in the bulk state

$$|\psi(\{j_e\})\rangle = \sum_{\iota_v}\hat{\psi}^{\{j_e\}}_{\{\iota_v\}}\bigotimes_v|\{\iota_v\}\rangle. \tag{10}$$

The coefficients $\hat{\psi}^{\{j_e\}}_{\{\iota_v\}}$ encode the quantum correlations among intertwiners.

III. SPIN NETWORKS WITH BOUNDARY AND NONTRIVIAL TOPOLOGY

Imagine cutting a generic *bounded* region R out of quantum 3D space. The corresponding state will be defined with support on an *open* graph $\gamma_R \subset \gamma$, which we can take to be comprised of the sets of vertices $\mathcal{V}_R$ and edges $\mathcal{E}_R$, with $|\mathcal{V}_R| = V_R$ the number of vertices and $|\mathcal{E}_R| = E_R$ the number of edges respectively. The *boundary* of R, ∂R, is the set $\mathcal{E}_{\partial R}$ of $E_{\partial R}$ edges which have only one end attached to a vertex laying in R. Such boundary edges are characterized by an open (uncontracted) dangling index m, while bulk edges connecting vertices within R are fully contracted. For states with support on open graphs, the contraction in (9) defines a *mapping* of the state $|\psi\rangle \in H_{V_R}$ on the boundary space of uncontracted indices,

$$H_{\partial R} = \bigoplus_{\{j_e\}}\bigotimes_{e\in\mathcal{E}_{\partial R}} V^{j_e}. \tag{11}$$

In particular, the gauge invariant property of the LQG wave functions defined on closed graphs reduces to a $SU(2)$-covariance of the bounded region wave function

$$\psi_R(\{g_e\}_{e\in\mathcal{E}}) = \psi_R(\{g_e h_{s(e)^{-1}}\}_{e\in\mathcal{E}_{\partial R}}). \tag{12}$$

In the boundary mapping, the information on the bulk holonomies, as well as the correlation structure of $\psi \in H_{V_R}$ gets encoded in the coefficients of the resulting boundary state $|\psi_R\rangle$. We are interested in the information concerning the *bulk curvature* and, in particular, in the way this affects (gets reflected in) the correlation structure of the boundary state $|\psi_R\rangle$.

Bulk curvature is generally associated to the presence of loops of nontrivial holonomies in the graph. However, the topology of the graph is only partially relevant to characterize such a degree of freedom. Indeed, thanks to the local gauge invariance of ψ_R, the structure of the bulk of γ_R can be drastically simplified via a partial gauge fixing of the bulk holonomies [46,73,74]. In particular, for any open region R, the gauge-invariant Hilbert space on γ_R is isomorphic to the gauge-invariant reduced space defined on a new graph Γ_R consisting of a single vertex intertwining the external edges of the boundary ∂R together with a number of (independent) loops L fixed by the combinatorics of the region, that is $L = E_R - V_R + 1$. If $L = 0$ there are no loops and γ_R has trivial topology. In particular, this implies that R has vanishing *intrinsic* curvature.

More generally, the Hilbert space of the reduced graph γ_R will consist of the intertwiner space of the single bulk vertex times the product of the boundary representations spaces, that is

$$H_{\gamma_R} = L^2[SU(2)^{\times(E+2L)}/SU(2)] = \bigoplus_{\{j_{\ell,e}\}}\left(H_v^L \otimes \bigotimes_{e\in\mathcal{E}_{\partial R}} V^{j_e}\right), \tag{13}$$

where the degeneracy space at the vertex now also involves the irreps on the loop

$$H_v^L \equiv \mathrm{Inv}_{SU(2)}\left[\bigotimes_{\ell=1}^{L}(V^{j_\ell}\otimes\bar{V}^{j_\ell})\otimes\bigotimes_{e\in\mathcal{E}_{\partial R}} V^{j_e}\right]. \tag{14}$$

The space in (13) provides a very concise description of the region R in terms of a single "loopy" vertex with both its boundary degrees of freedom and bulk nontrivial holonomies. The gauge reduction isomorphism does not produce

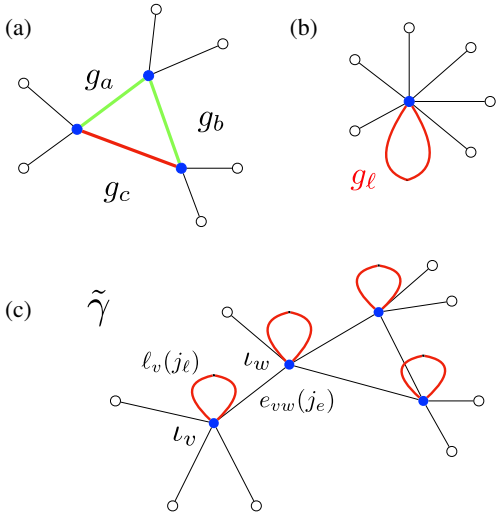

FIG. 2. (a) Reduction by gauge fixing of the holonomies along the maximal spanning tree connecting three vertices of an open spin network. (b) Resulting nontrivial holonomy on a loop attached to a coarse-grained vertex. (c) Bounded quantum 3*D* region with uniformly distributed loops realized as the gluing of a set of coarse-grained vertices.

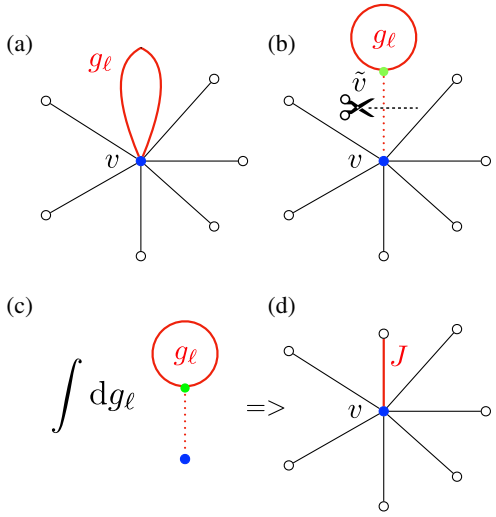

FIG. 3. (a) A single loopy vertex. (b) Vertex unfolding: isolate the nontrivial loop holonomy. (c) Partial trace via integration over the loop holonomy. (d) Tagged vertex.

any coarse graining on physical degrees of freedom. Nevertheless, partial information on the combinatorics of the reduced graph is lost. As a consequence, the correspondence between the original graph and its flower is many-to-one [74].

Now, imagine operating a similar reduction by gauge fixing on a *collection* of subregions, so as to end up with a set of loopy vertices glued together via edges dressed with a trivial holonomy. In this way, we can construct a new spin-network state with support on an open graph $\tilde{\gamma}_R$ associated to an extended 3*D* space region with distributed *intrinsic* curvature (see Fig. 2).

Such an intermediate level of description allows one to localize and keep track of the nontrivial holonomies $\{g_\ell\}$ (classically closure defects) responsible for the curvature at the vertices of the graph, without trivializing the topology of the graph, which is going to play a role in the entanglement structure of the boundary.

IV. TAGS FROM SPIN-NETWORK KIRIGAMI

Along this line, let us consider for simplicity the case of a uniformly curved region of quantum 3*D* space, given by an open-graph state $|\psi_R\rangle = |\psi_R(\{g_\ell\})\rangle$ with all V_R vertices carrying one single loop holonomy g_ℓ. Further, let us assume for now that each vertex can have at most one open edge. This very simplified setting is what we need to neatly separate boundary from bulk degrees of freedom, as shown in Fig. 3. The first step in this sense consists of integrating out the loop holonomies. Following [86], for each spin k carried by the loop, one can separate the loop from the edges at each vertex by unfolding the intertwiner into two different intertwiners connected by a virtual link labeled by an intermediate spin J: one intertwiner recoupling the boundary edges spins j_e at v into J and a second three-valent intertwiner recoupling the two copies of the spin k into J at the virtual vertex $\tilde{v}$. Accordingly, the intertwiner space in (14) now decomposes as

$$H_v^L = \bigoplus_{J,\{k\}} \left\{ \mathrm{Inv}_{SU(2)} \left[\bigotimes_{e\in v} V^{j_e} \otimes V^J \right] \otimes \mathrm{Inv}_{SU(2)} [V^J \otimes (V^k \otimes \bar{V}^k)] \right\}. \quad (15)$$

A basis in H_v^L is given by (see for instance [87])

$$|J, k, \iota, \{j_e\}[g_\ell]\rangle = D^k(g_\ell) C^{k,J|k}_{\tilde{m},M|m} \langle J, M|\iota\rangle \quad (16)$$

with

$$C^{k,J|k}_{\tilde{m},M|m} = \langle k, m|(k, \tilde{m}) \otimes (J, M)\rangle \quad (17)$$

the Clebsh-Gordan coefficient associated to the three-valent intertwiner at $\tilde{v}$.

At each vertex of the graph, the integration over the loop holonomy only involves the Clebsh-Gordan coefficient and the Wigner matrix of the loop at the level of the basis in (16). One can then compute the vertex density matrix ρ_k as

$$\rho_k = \int \mathrm{d}g_\ell |J, k, \iota, \{j_e\}[g_\ell]\rangle\langle J, k, \iota, \{j_e\}[g_\ell]| \quad (18)$$

and show that the sum of ρ_k over the loop spin k gives exactly the identity matrix $\rho = \langle J, M|\iota\rangle\langle\iota|J, M\rangle$, with $|\tau\rangle = \langle J, M|\iota\rangle$ a *basis* in the *reduced* vertex space [87]

$$H_v^J = V^J \otimes M_J^{\{j_e\}}, \tag{19}$$

with $M_J^{\{j_e\}} \equiv \mathrm{Inv}_{SU(2)}[V^J \otimes\otimes_{e\in v} V^{j_e}]$.

As a result of the integration, curvature is locally encoded into a virtual spin J, or *tag*, attached to the vertex. We can see the vector $|J, M\rangle \in V^J$ as the result of the recoupling of all the spins j_e at the vertex into a nonvanishing overall spin J, a topological defect which breaks local gauge invariance.[1]

Starting from the tagged intertwiner description, we now define a *uniformly curved* quantum $3D$ bounded space geometry as the *extended* boundary map

$$|\psi_\tau\rangle = \sum_{\{j_e\}} \left(\bigotimes_{e=1}^{E} \langle e(g_e)| \right) |\psi_b\rangle \tag{21}$$

where the generic tagged state $|\psi_b\rangle$ is defined, for fixed spins $\{J, j_e\}_v$, as

$$|\psi_b\rangle = \sum_{\{M_v\}\{\iota_v\}} \widehat{\psi_b}^{\{J,j_e\}}_{\{M_v\},\{\iota_v\}} \bigotimes_{v\in\mathcal{V}_R} |\tau_v\rangle \tag{22}$$

in the tensor product space of V_R tagged intertwiner spaces $H_{V_R} \equiv \otimes_v^{V_R} H_v^{J_v}$. Differently from (9), the projected state now lives in an *extended* boundary space,

$$H_\tau \equiv \bigoplus_{\{J,j_e\}} \bigotimes_{v\in\mathcal{V}_R} V^{J_v} \otimes \bigotimes_{e\in\mathcal{E}_{\partial R}} V^{j_e} \tag{23}$$

which comprises the tensor product of tags and boundary-spin representation spaces.[2]

On the extended boundary, the tagged open graph state is written as

$$|\psi_\tau\rangle = \sum_{\{M_v,m_e\}} \hat{\psi}_\tau^{\{J_v,j_e\},\{\iota_v\}}{}_{\{M_v,m_e\}} \bigotimes_{v\in\mathcal{V}_R} |J_v, M_v\rangle \bigotimes_{e\in\mathcal{E}_{\partial R}} |j_e, m_e\rangle, \tag{24}$$

with coefficients $\hat{\psi}_\tau^{\{J_v,j_e\},\{\iota_v\}}{}_{\{M_v,m_e\}}$ encoding the information on the quantum correlations among bulk intertwiners, the connectivity, and the topological defects of the graph. We expect states in (24) to be generically highly entangled, with information about bulk geometry encoded into the boundary state coefficients $\mathcal{C}$ in a complicated way. In the extended boundary system, such information is shared by boundary spins and bulk tags.

Now, consider an observer having access only to the external boundary system. Such an observer cannot measure the information on the bulk. In the following analysis, we describe such a coarse-grained viewpoint of the boundary observer by introducing a *random measurement* on the state $|\psi_\tau\rangle$ and proceed to investigate the boundary-system/bulk-environment coupling via a combination of random projections and partial tracing over the tags.

V. NEGATIVITY OF A TRIPARTITE BOUNDARY-TAGS SYSTEM

Let us consider the extended boundary space (23). For convenience, let us assume curvature quantified by the tags to be uniformly and homogeneously distributed throughout the graph $\tilde{\gamma}_R$. This amounts to having a tag for each vertex of the graph while setting all the spins $\{j_e\}$ and $\{J_v\}$ to be equal to the single value j and J respectively, generally with $j \neq J$. In particular, this implies we are turning off the direct sum over the spins $\{J, j_e\}$ in (23). This allows us to work with a factorized Hilbert space, while disregarding the correlations among different spin sectors of the full quantum geometry wave function (see, e.g., [29,88] on the role of such correlations).

A *random measurement* on the bulk state $|\psi_b\rangle$, prepared on $\otimes_v H_v^J$, is realized by a projection onto a set of independent and individual (Haar) random vertex states $|f_v\rangle$ in the *extended* vertex space

$$K_v^J = V^J \otimes \bigotimes_{j_e\in v} V^{j_e} \otimes M_J^{\{j_e\}}, \tag{25}$$

which comprises the intertwiner space at the vertex, the spin irrep spaces of the edges connecting the vertex with the rest of the graph, as well as the tag spin space. In particular, we can obtain the state $|f_v\rangle$ by acting on a reference state $|0\rangle$ in K_v^J at v with a Haar random unitary, that is $|f_v\rangle = U_v|0\rangle$ [67].

The generic random vertex state is explicitly written as

$$|f_v\rangle = \sum_{\iota_v,\{n_e\}} f^v_{\iota_v,\{n_e\}} \langle J, M|\iota_v\rangle \otimes \bigotimes_{e\in v} |j_e, n_e\rangle. \tag{26}$$

The randomized extended boundary density matrix is then simply defined along with (21) by a trace over bulk indices, which contract $\rho_b = |\psi_b\rangle\langle\psi_b|$ and $\rho_E = |E\rangle\langle E|$, for $|E\rangle = \otimes_e^E |e\rangle$, with the further insertion of the *random projector* $\Pi = \otimes_v^{V_R} \Pi_v = \otimes_v^{V_R} |f_v\rangle\langle f_v|$:

$$\rho_\tau = \mathrm{Tr}[\rho_b \otimes \rho_E \Pi]. \tag{27}$$

[1]Given a tagged basis $|\tau_v\rangle$ at each vertex, we can define a *tagged spin network* basis

$$|\gamma, \{j_e\}, \{\iota_v\}, \{J_v\}\rangle = \left(\bigotimes_{e=1}^{E} \langle e(g_e)| \right) |\{\tau_v\}\rangle \tag{20}$$

for the whole state on $\tilde{\gamma}_R(V_R, E_R, E_{\partial R})$.

[2]In fact, one can think of the tag factor in (23) as a disjoint *inner* boundary associated to closure defects at the bulk vertex. This is compatible with a picture of the tags as the result of a set of holes cut out of a planar spin network punctured by uncontracted bulk edges. In the standard picture, such holes correspond to loops which recouple the puncturing edges.

The bulk state ρ_b and the maximally entangled edge state ρ_E enter as product states in the trace, while the information on the tags is enclosed in the bulk state.

Let us define now a tripartition of the extended boundary system into three subsystems A_1, A_2, B, with A_1, A_2 complementary regions of the external boundary, and B the set of tags in the bulk, as depicted in Fig. 4. This corresponds to the following factorization of the extended boundary Hilbert space at fixed spins:

$$H_\tau = \bigotimes_{e\in A_1} V^{j_e} \otimes \bigotimes_{e\in A_2} V^{j_e} \otimes \bigotimes_{i\in B} V^{J_i}. \tag{28}$$

Starting from (28), we focus on the reduced state obtained tracing over the tag spins in B,

$$\rho_{A_1A_2} = \mathrm{Tr}_B[\rho_\tau]. \tag{29}$$

As anticipated in Sec. I, the amount of entanglement of the state can be quantified by counting the number of negative eigenvalues of the partial transpose of the reduced state $\rho_{A_1A_2}^{T_{A_2}}$ [77], via a measure of logarithmic negativity defined as

$$E_N(\rho_{A_1A_2}) \equiv \log \|\rho_{A_1A_2}^{T_{A_2}}\|_1. \tag{30}$$

In order to compute (30), the first key ingredient is to first look at the kth Rényi negativity of $\rho_{A_1A_2}$,[3]

$$N_k(\rho_{A_1A_2}) = \mathrm{Tr}[(\rho_{A_1A_2}^{T_{A_2}})^k/(\mathrm{Tr}[\rho_{A_1A_2}])^k], \tag{31}$$

hence, eventually recovering the logarithmic negativity by taking the $k\to 1$ limit of the logarithm of the analytic continuation of the momenta for even k [69]. In particular, since we took a random measurement on the bulk state, we will need to compute the Rènyi negativity in *expected value*, with respect to the uniform Haar measure μ, namely

$$\mathbb{E}_\mu[N_k(\rho_{A_1A_2})] \equiv \overline{N_k(\rho_{A_1A_2})}. \tag{32}$$

Following [61,67,69], we know that, due to concentration of the trace, a regime of large spins allows us to approximate the Rènyi negativity by the ratio of expected values of the kth moment and the kth power of the partition function of $\rho_{A_1A_2}^{T_{A_2}}$, that is

$$\overline{N_k(\rho_{A_1A_2})} \simeq \frac{\overline{\mathrm{Tr}[(\rho_{A_1A_2}^{T_{A_2}})^k]}}{(\mathrm{Tr}[(\rho_{A_1A_2})])^k} \equiv \frac{\overline{Z_1^{(k)}}}{Z_0^{(k)}}. \tag{33}$$

[3]Notice that the trace operation Tr in (31) now involves sums over boundary indices (dangling edges and tags). The denominator in (31) directly comes from the normalization of ρ_{AA_2}.

Moreover, in the large spin regime, we have

$$N_k(\rho_{A_1A_2}) \simeq \overline{N_k(\rho_{A_1A_2})}, \tag{34}$$

that is, the function is well approximated by its *typical value*.

The expected values of the partition functions in (33) are computed via the standard *replica* technique. We first linearize the partial transpose matrix as follows:

$$\begin{aligned}\mathrm{Tr}[(\rho_{A_1A_2}^{T_{A_2}})^k] &= \mathrm{Tr}[\rho_{A_1A_2}^{\otimes k} P_{A_1}(X)\otimes P_{A_2}(X^{-1})] \\ &= \mathrm{Tr}[\rho_R^{\otimes k} P_{A_1}(X)\otimes P_{A_2}(X^{-1})\otimes P_B(\mathbb{1})].\end{aligned} \tag{35}$$

Here, we generally denote $P_I(\sigma)$ as a unitary representation of the permutation σ, $I = A_1, A_2, B$, with X, X^{-1} and $\mathbb{1}$ the cyclic, anticyclic, and identity permutations. On the spins' and tags' dangling indices, the operator $P_B(\mathbb{1})$ realizes the partial trace over the tags on ρ_b, while $P_{A_1}(X)\otimes P_{A_2}(X^{-1})$ act on the k copies of uncontracted spins in $\rho_E^{\otimes k}$ implementing the replica trick and the partial transposition respectively.

For the linearity of the trace, the expectation value can be carried out before taking the trace, and it will concern only the random tensors. From (27), we have

$$\begin{aligned}\overline{Z_1^{(k)}} &= \mathrm{Tr}\left[\rho_b^{\otimes k}\otimes\rho_E^{\otimes k}\left(\bigotimes_v \overline{(|f_v\rangle\langle f_v|)^{\otimes k}}\right)\right. \\ &\qquad \left.\cdot P_{A_1}(X)\otimes P_{A_2}(X^{-1})\otimes P_B(\mathbb{1})\right], \\ \overline{Z_0^{(k)}} &= \mathrm{Tr}\left[\rho_b^{\otimes k}\otimes\rho_E^{\otimes k}\left(\bigotimes_v \overline{(|f_v\rangle\langle f_v|)^{\otimes k}}\right)\right],\end{aligned} \tag{36}$$

where the overall trace now runs over both bulk and boundary indices.

By Schur's lemma, the average of the k copies of the vertex state in (36) results in a sum over unitary representations of the permutation group g_v acting on the k copies of the extended vertex space K_v^J [61,69,71],

$$\overline{(|f_v\rangle\langle f_v|)^{\otimes k}} = \frac{(D_v-1)!}{(D_v+k-1)!}\sum_{g_v\in S_k} P_v(g_v), \tag{37}$$

with dimension $D_v = \dim(K_v^J)$.

By performing the average individually on each independent random vertex, we obtain[4]

[4]$\overline{Z_0^{(k)}}$ has the same form with X and X^{-1} replaced by $\mathbb{1}$.

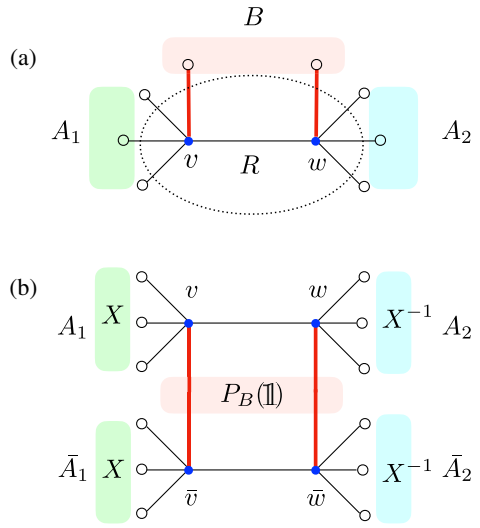

FIG. 4. (a) Tripartition of the spin-network extended boundary for a simple graph comprised of two four-valent vertices glued via an edge. (b) Partial tracing of the density matrix over the tags' space.

$$\overline{Z_1^{(k)}} = \mathcal{C}\Big[\rho_b^{\otimes k} \otimes \rho_E^{\otimes k}\Big(\bigotimes_v \sum_{g_v \in S_k} P_v(g_v)\Big) \cdot P_{A_1}(X) \otimes P_{A_2}(X^{-1}) \otimes P_B(\mathbb{1})\Big], \tag{38}$$

with $\mathcal{C} = \prod_v \left[\frac{(D_v-1)!}{(D_v+k-1)!}\right]$.

On the bulk indices at each vertex, the permutation operator $P_v(g_v)$ factorizes into *four* independent operators (see Fig. 5),

$$P_v(g_v) = P_{v,0}(g_v) \otimes \bigotimes_{e^i_{vw}\in\mathcal{E}_R} P_{v,i}(g_v) \otimes \bigotimes_{e^i_{v\bar{v}}\in\mathcal{E}_{\partial R}} P_{v,i}(g_v) \otimes P_{v,\tau}(g_v), \tag{39}$$

where $P_{v,0}(g_v)$ acts on k copies of the multiplicity intertwiner space, $\otimes_{e^i_{vw}\in\mathcal{E}_R} P_{v,i}(g_v)$ acts on k copies of the internal edges, $\otimes_{e^i_{v\bar{v}}\in\mathcal{E}_{\partial R}} P_{v,i}(g_v)$ acts on the boundary semiedges,[5] and finally $P_{v,\tau}(g_v)$ acts on k copies of the *recoupled tag spin at the vertex*.

Accordingly, the trace in (38) factorizes over the Hilbert spaces of (a) internal edges, (b) boundary spins, (c) tag spins, and (d) bulk intertwiners. As a result, we can eventually rewrite the kth power of the normalized partition function in (33) as

[5]We indicate by $\bar{v}$ a virtual vertex connected to v by the open boundary edge $e^i_{v\bar{v}}$.

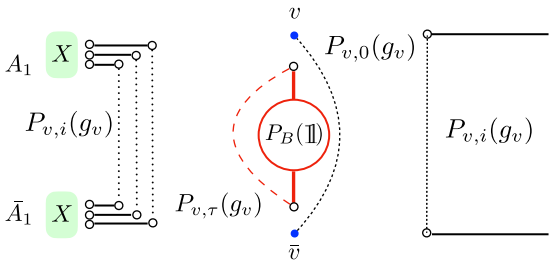

FIG. 5. Permutation operator $P_v(g_v)$ action factorizes on the indices of the extended vertex state. In the example in the figure the operator acts as the identity connecting the set of internal indices of v to the same set in $\bar{v}$, while $P_B(\mathbb{1})$ realizes the partial trace over the tags.

$$\frac{\overline{Z_1^{(k)}}}{\overline{Z_0^{(k)}}} = \sum_{\{g_v\}} e^{-A^{(k)}_{1/0}}, \tag{40}$$

where $A^{(k)}_{1/0} \equiv A^{(k)}_1/A^{(k)}_0$ defines the (normalized)[6] action of a classical *generalized* Ising-like model:

$$A^{(k)}_1[\{g_v\}] = A_b + \xi + \sum_{e^i_{vw}\in\mathcal{E}_R} \Delta(g_v, g_w) \log d_{j^i_{vw}} + \sum_{e^i_{v\bar{v}}\in A_1} \Delta(g_v, X) \log d_{j^i_{v\bar{v}}} + \sum_{e^i_{v\bar{v}}\in A_2} \Delta(g_v, X^{-1}) \log d_{j^i_{v\bar{v}}}, \tag{42}$$

with ξ a constant term and

$$A_b = -\log\Big\{\mathrm{Tr}\Big[\rho_b^{\otimes k} \otimes P_B(\mathbb{1}) \cdot \Big(\bigotimes_v P_{v,0}(g_v) \otimes P_{v,\tau}(g_v)\Big)\Big]\Big\} \tag{43}$$

the bulk state contribution to the action, which accounts for the presence of the curvature measured by the tag term in ρ_b. In the analogy, the *generalized spins* correspond to the permutation operators $P_v(g_v)$ sitting on the vertices of the open spin network graph $\tilde{\gamma}_R$ acting on the k replicas of the vertex indices space. The permutation fields X, X^{-1}, and $\mathbb{1}$ play the role of boundary conditions set on the virtual one-valent vertices ($\bar{v}$) attached to the dangling spins and tags of the extended boundary.

The two-body interaction terms measure the length of the permutation loops across the replicas, weighted by the (log of the) dimension of the representation carried by the edges

[6]with

$$A^{(k)}_0 = \sum_{e^i_{vw}\in\mathcal{E}_R} \Delta(g_v, g_w) \log d_{j^i_{vw}} + \sum_{e^i_{v\bar{v}}\in A_1\cup A_2} \Delta(g_v, \mathbb{1}) \log d_{j^i_{v\bar{v}}} + A_b + \xi. \tag{41}$$

of the graph. These lengths are conveniently described as Cayley distances $\Delta(g,h) = k - \chi(g^{-1}h)$ on the permutation group S_k, where $\chi(g)$ indicates the number of cycles in a permutation g [61,69].[7]

The calculation of typical value of Rényi negativity is then mapped to the minimization of the action (42). In general, the three boundary conditions will propagate inside the spin network graph $\tilde{\gamma}_R$. Depending on the couplings and the connectivity of the graph, different configurations of the model will be associated to different sets of domains for $X, X^{-1}, \mathbb{1}$ in the bulk. As usual, we expect maximal domains to be associated to equilibrium configurations. In particular, maximal domains correspond to minimal domain walls.

By describing interactions via a Cayley distance we see that the Rényi negativity should depend directly on the *area* of such minimal domain walls in the network, given by the number of edges of $\tilde{\gamma}_R$ associated to a nonvanishing Cayley distance between permutations in the two domains. In particular, thanks to the existence of a well-defined loop quantum gravity area operator acting on the edges of the spin network, we can map domain wall areas to actual quantum geometry surfaces in our $3D$ space region R.

VI. GENERALIZED ISING MODEL: MODELING BULK CONTRIBUTIONS

The tensor product form of the edges and bulk density matrices in (38) corresponds to a factorization of the typical Rényi negativity into a combinatorial contribution associated to the distribution of maximally entangled edge states e_{vw} and a bulk contribution carrying physical correlations among intertwiners. The latter, in particular, contains the information on the intrinsic curvature of the $3D$ geometry, in the form of tags, as apparent from (22). We would expect such information to be highly mixed in the bulk. However, after the partial tracing over the loop holonomies, the $SU(2)$ covariance of the tagged-bulk state induces $SU(2)$ invariance on the associated density matrix, which necessarily reads as a tensor product for fixed tag spins $\{J_v\}$, that is

$$\rho_b = \bigotimes_v^{V_R} \frac{\mathbb{1}}{2J_v+1} \otimes \rho_{\{J_v\}}, \tag{44}$$

which corresponds to a totally mixed state on the tags' space and a generally nontrivial density matrix $\rho_{\{J_v\}} \in \mathrm{End}[H_{V_R}]$ [87,89].

From the form of ρ_b in (44), we have

$$\rho_b^{\otimes k} = \bigotimes_{v=1}^{V_R} \left(\frac{\mathbb{1}}{2J_v+1}\right)^{\otimes k} \otimes \rho_{\{J_v\}}^{\otimes k}; \tag{45}$$

then the bulk term A_b generally factorizes as follows:

$$\begin{aligned} A_b &= -\log\left\{\left[\rho_{\{J_v\}}^{\otimes k} \otimes \bigotimes_v \left(\frac{\mathbb{1}}{2J_v+1}\right)^{\otimes k} \right.\right. \\ &\quad \left.\left. \otimes P_B(\mathbb{1})\left(\bigotimes_v P_{v,0}(g_v) \otimes P_{v,\tau}(g_v)\right)\right]\right\} \\ &= A_\iota + A_\tau \end{aligned} \tag{46}$$

with a bulk intertwiner contribution A_ι defined as

$$A_\iota \equiv -\log\{\mathrm{Tr}[\rho_{\{J_v\}}^{\otimes k}(\otimes_v P_{v,0}(g_v))]\}, \tag{47}$$

and a contribution of the tags, A_τ, given by

$$A_\tau \equiv -\log\left\{\mathrm{Tr}\left[\bigotimes_v \left(\frac{\mathbb{1}}{D_{J_v}}\right)^{\otimes k} \otimes P_B(\mathbb{1}) \cdot (\otimes_v P_{v,\tau}(g_v))\right]\right\}, \tag{48}$$

where we used $D_{J_v} = 2J_v + 1$, the dimension of the tag space. The result of the trace in (48) is

$$\begin{aligned} &\left(\prod_{v\in\mathcal{V}_R} D_{J_v}^{-k}\right)\mathrm{Tr}\left[\bigotimes_{\langle v\tilde{v}\rangle}\left(\sum_{g_v\in S_k} P_v(g_v)\right) \otimes P_B(\mathbb{1})\right] \\ &\quad = \sum_{\{g_v\}}\prod_v D_{J_v}^{-\Delta(g_v,\mathbb{1})}. \end{aligned} \tag{49}$$

Therefore, the tags' contribution to the action reads as

$$A_\tau = \sum_v \Delta(g_v,\mathbb{1}) \log D_{J_v}, \tag{50}$$

which ends up being equivalent to a pairwise interaction term from an inner edge. The full action can be written as

$$\begin{aligned} A_1^{(k)} &= \xi + A_\iota + \sum_{e^i_{vw}\in\mathcal{E}_R} \Delta(g_v,g_w)\log d_{j^i_{vw}} \\ &\quad + \sum_{e^i_{v\tilde{v}}\in A_1} \Delta(g_v,X)\log d_{j^i_v} + \sum_{e^i_{v\tilde{v}}\in A_2} \Delta(g_v,X^{-1})\log d_{j^i_v} \\ &\quad + \sum_v \Delta(g_v,\mathbb{1})\log D_{J_v}. \end{aligned} \tag{51}$$

The bulk contribution A_ι is nontrivial as long as the bulk intertwiners are correlated. In fact, it vanishes only if we consider ρ_{J_v} to be a pure product state in $\mathrm{End}[H_{V_R}]$ as shown in [61]. On the other hand, both edge and tag contributions have to do with the topology of the graphs' support $\tilde{\gamma}_R$, connectivity, and topological defects respectively.

As a general result of our analysis, we can then formally divide the action in three terms as follows:

[7]This is k for the identity and 1 for a k cycle. Then, we see that $\Delta(g,h)$ gives the minimal number of swaps to go from g to h, for $g,h \in S_k$.

$$A_1^{(k)} = A_{\text{topology}}^{(k)} + A_{\text{phys}}^{(k)} \tag{52}$$

with $A_{\text{topology}}^{(k)} = A_{\text{edges}}^{(k)} + A_{\text{tags}}^{(k)}$ and $A_{\text{phys}} = A_\iota$ referring to the physical quantum correlations among bulk intertwiners.

In the following analysis, we will consider the case where the intertwiners' contribution is small, thereby looking at the correlations induced solely by the combinatorial structure of the graph, with a focus on the role of the tags. We leave the study of the intertwiners' contribution in this setting for future work.

VII. LOGARITHMIC NEGATIVITY AND ENTANGLEMENT PHASES

By neglecting A_ι, we are left with action $A_1^{(k)}$ with two-body interactions only, which favors neighboring "spins" to be parallel. Given $d_j = 2j+1$ and $D_J = 2J+1$ the dimension of edge spins and tag Hilbert space respectively, we define

$$\log d_j \equiv \beta, \qquad \log D_J \equiv \beta_t \tag{53}$$

as the interaction strengths intended as inverse temperatures, in analogy with the Ising model. Thereby, we can rewrite the action $A_{\text{topology}}^{(k)}$ as

$$\begin{aligned} A_{\text{topology}}^{(k)} &= \beta\Bigg[\sum_{e_{vw}^i \in \mathcal{E}_R} \Delta(g_v, g_w) + \sum_{e_{v\bar{v}}^i \in A_1} \Delta(g_v, X) \\ &\quad + \sum_{e_{v\bar{v}}^i \in A_2} \Delta(g_v, X^{-1})\Bigg] + \beta_t \sum_{v \in \mathcal{V}_R} \Delta(g_v, \mathbb{1}) \\ &= \beta H_e + \beta_t H_{\text{tags}}, \end{aligned} \tag{54}$$

with generalized Hamiltonians H_e, H_{tags} expressing the energy cost of the configuration. In general, we expect that the boundary conditions X, X^{-1}, and 1 percolate inside the network, flipping the generalized spins on the bulk vertices. This creates some internal domains filled with one of the three boundary conditions. Nonvanishing contributions to the action come from edges that connect different domains, which will be related to a nonzero Cayley distance. Given

$$N_k(\rho_{A_1A_2}) \simeq \sum_{\{g_v\}} e^{-A_{\text{topology}/0}^{(k)}}, \tag{55}$$

in the large spin (the strong coupling or "low temperature") regime, the leading contribution to N_k corresponds to dominant $\{g_v\}$ configurations that minimize the action. Such configurations correspond to maximal uniform spin domains separated by extremal domain walls which minimize the energy cost (minimal surface areas) [61].

Concretely, we then proceed with minimizing the action in (54) via a heuristic argument based on the property of the Cayley distance on the permutation group S_k. Given two permutations $g, h \in S_k$, the Cayley distance $\Delta(g,h)$ defines a metric on the group, corresponding to the minimum number of swaps acting on g to give h. For some special permutations, the Cayley distance depends nicely on the order of the group k. For example, in the case of the (anti-) cyclic permutations we deal with, we have

$$\Delta(\mathbb{1}, X) = \Delta(\mathbb{1}, X^{-1}) = k-1 \tag{56}$$

$$\Delta(X, X^{-1}) = \begin{cases} k-1, & k \text{ odd} \\ k-2, & k \text{ even} \end{cases}. \tag{57}$$

With this metric, we can define a geodesic on the group S_k between g and k as the set of permutations $\{\pi\}$ such that

$$\Delta(g,\pi) + \Delta(\pi, h) = \Delta(g,h). \tag{58}$$

In particular, it is known that the set of permutations that are simultaneously geodesics between X, X^{-1}, and 1 exist, and it is in a bijection with the set of noncrossing partitions $NC(k)$ of the set $\{1,\ldots,k\}$, with cardinality given by the Catalan numbers C_k [69]. Defining by τ the permutations on such geodesics, we have that

$$\Delta(\mathbb{1}, \tau) = \left\lfloor \frac{k}{2} \right\rfloor, \quad \Delta(X,\tau) = \Delta(X^{-1},\tau) = \left\lceil \frac{k}{2} \right\rceil - 1. \tag{59}$$

Given the homogeneity of our states, the minimization of the energy costs amounts to a minimization of the Cayley distances between any pairs of connected vertices.

Let us consider a single vertex v. To such a vertex the random averaging assigns a permutation element g_v, which will eventually interact with the three permutations we choose as boundary conditions, namely X, X^{-1}, and 1. Recalling the symmetry between X and X^{-1}, we expect that only *three* possible *minimal energy* configurations can result from such an interaction:

(1) $g_v = X, X^{-1}$, in which case we minimize the distance between the vertex v and the neighboring vertices respectively contained in the X or X^{-1} domain;
(2) $g_v = \mathbb{1}$, in which case we minimize the distance between the vertex v and the neighboring vertices contained in the 1 domain;
(3) $g_v = \tau$, in which we minimize simultaneously the distance between the X, X^{-1}, and the 1 domains.

Notice that the latter case is peculiar to the tripartite model only, since it can occur only when all three permutations interact in a single vertex [61,67,69].

A. Example: Cluster of four tags

Let us consider the example of an open spin network state with support on a graph $\tilde{\gamma}_R$ with $E_{\partial R} = 4$ boundary edges, and $V_R = 4$ tagged four-valent vertices in the bulk

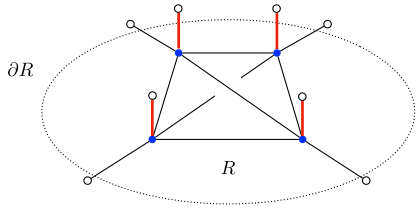

FIG. 6. Example: tagged open spin network graph corresponding to a cluster of four-valent tagged vertices, with $T = 4$ and $E_{\partial R} = 4$.

(see Fig. 6). In the following we indicate with T the number of tags, which in the present case is equal to the number of vertices, namely $T = V_R$. We refer to this setting as a *cluster of tags*, corresponding to a uniformly curved quantum $3D$ space region R. Via random averaging, we get four permutations operators on the spin network, one for each tagged vertex. Following the discussion above, we have three possible configurations with minimal energy. The corresponding actions (for even $k > 0$) read as the following:

(1) A cluster colored with $X(X^{-1})$:

$$\mathcal{A}_k^{(X)} = \beta S(k-2) + \beta_t T(k-1). \tag{60}$$

Here S is the *minimal* number of edge cuts comprising the surface separating two domains with X and X^{-1}.

(2) A cluster colored with $\mathbb{1}$:

$$\mathcal{A}_k^{(\mathbb{1})} = \beta E_{\partial R}(k-1). \tag{61}$$

(3) A cluster colored with τ:

$$\mathcal{A}_k^{(\tau)} = \beta E_{\partial R}\left(\frac{k}{2} - 1\right) + \beta_t T \frac{k}{2}. \tag{62}$$

Such configurations define the three *equilibrium phases* of our simple model, corresponding to three different entanglement regimes for the boundary state $\rho_{A_1A_2}$. The parameter space of such regimes is completely specified by the following three inequalities:

$$\mathcal{A}_k^{(\mathbb{1})} < \mathcal{A}_k^{(\tau)} \Leftrightarrow \beta E_{\partial R} < \beta_t T \tag{63}$$

$$\mathcal{A}_k^{(\tau)} < \mathcal{A}_k^{(X)} \Leftrightarrow \beta E_{\partial R} < \beta_t T + 2\beta S \tag{64}$$

$$\mathcal{A}_k^{(X)} < \mathcal{A}_k^{(\mathbb{1})} \Leftrightarrow \beta E_{\partial R} > \beta_t T + \beta S\left(1 - \frac{1}{k-1}\right), \tag{65}$$

where the last condition (65) is relevant to establish a hierarchy between the three configurations, while it does not play a role in the search for the minimal energy cost. Notably, this rules out from the parameter space the only condition which depends explicitly on the order of the permutation group k.

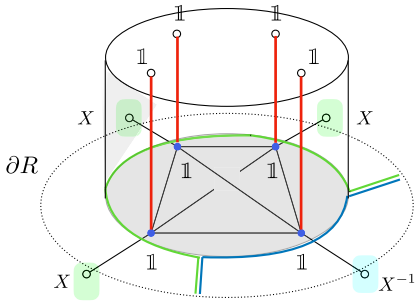

FIG. 7. Domain wall's configuration in the hole regime.

Consider the (positive definite) quantity $\beta E_{\partial R}$, namely the set of edges comprising the external surface of our $3D$ region weighted with the factor β. If $\beta E_{\partial R} < \beta_t T$, as $2\beta S > 0$, (64) is also satisfied; then $\mathcal{A}_k^{(\mathbb{1})} < \mathcal{A}_k^{(X)}, \mathcal{A}_k^{(\tau)}$. The configuration with a bulk colored with $g_v = \mathbb{1}\ \forall\ v$ dominates. In particular, this corresponds to the formation of a domain wall around the cluster of tags. The domain wall sharply divides the spin-network boundary from the bulk of the region R. We refer to such a regime as the *hole* regime (see Fig. 7). Notice that, due to the bound on the maximum dimension of the tag spin [74], in the present example we can have at most

$$J^{(\max)} = 4j \Rightarrow \beta_t^{(\max)} = \beta + \log 4. \tag{66}$$

Then, in a large spin regime, we can generally consider $\beta_t^{(\max)} \backsim \beta$. Therefore, in order for the *hole* regime condition to be verified we must have

$$T > E_{\partial R}. \tag{67}$$

More generally, the hole regime will be favored by tags recoupling a large number of edge spins, corresponding to the case of coarse-grained vertices with high valence.

When the number of tagged vertices in the bulk and boundary edges is balanced we exit the hole regime and we need to consider $\beta E_{\partial R} \in [\beta_t T, \beta_t T + 2\beta S]$. From Eq. (63), we see that in this range of values $\mathcal{A}_k^{(\tau)} < \mathcal{A}_k^{(\mathbb{1})}$. At the same time, Eq. (64) implies that $\mathcal{A}_k^{(\tau)} < \mathcal{A}_k^{(X)}$; hence the minimal configuration is the one in which the geodesic permutation τ takes all the bulk, with the action $\mathcal{A}_k^{(\tau)}$ dominating. We call this setting the *island* regime. The island domain wall stands between the three boundary condition domains preventing them from accessing the bulk of R (see Fig. 8). Differently from the hole regime, the connectivity of the graph is not canceled in this case. Tags and boundary spins are connected through the island.

Finally, for $\beta E_{\partial R} > \beta_t T + 2\beta S$, namely when the tag's environment is small compared with the boundary system, from Eqs. (63) and (64) it follows that $\mathcal{A}_k^{(X)} < \mathcal{A}_k^{(\mathbb{1})}, \mathcal{A}_k^{(\tau)}$. In this regime, the minimal energy configuration is associated

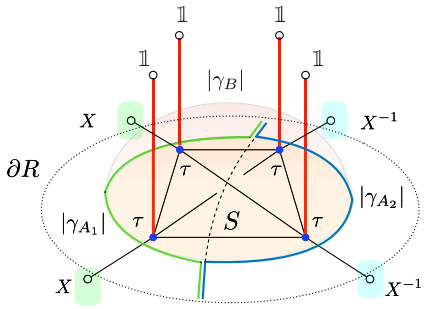

FIG. 8. Domain walls' configuration in the island regime.

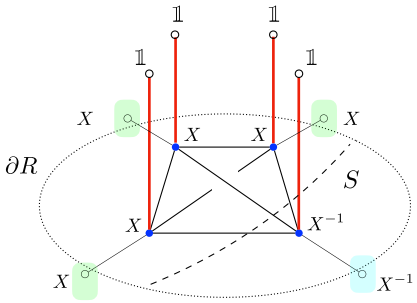

FIG. 9. Domain wall's configuration in the bipartite regime.

to an effective bipartition of R into two domains, one colored with the X permutation and the other with the X^{-1} permutation (see Fig. 9).[8] We refer to this setting as the *bipartite* regime.

B. Entanglement phases

We can now compute the typical logarithmic negativity of the random mixed state $\rho_{A_1A_2}$ in the three regimes considered in the given example.

In the hole regime, from the action in (61), we get

$$E_N^{(\text{hole})}(\rho_{A_1A_2}) \simeq -\lim_{k\to 1}\mathcal{A}_k^{(\mathbb{1})} = -\lim_{k\to 1}\beta E_{\partial R}(k-1) = 0. \quad (68)$$

A vanishing negativity tells us that the boundary state has positive partial transpose (PPT); hence, according to the Peres criterion [76], that boundary state could be separable. This suggests that $\rho_{A_1A_2}$ is well described by a maximally mixed state. The boundary system is almost fully entangled with the large number of degrees of freedom environment with little quantum correlation between A_1 and A_2. This effectively corresponds to a thermalization of the boundary state, in strong analogy with the results in [72,90], where the typicality of the random state, in the large spin regime, similarly played a crucial role.

Moving to the island regime, the *minimal* action reads as

$$\mathcal{A}_k^{(\tau)} = \beta E_{\partial R}\left(\frac{k}{2}-1\right) + \beta_t T\frac{k}{2}, \quad (69)$$

and the typical value of the logarithmic negativity in the $k\to 1$ limit is given by

$$\begin{aligned} E_N^{(\text{island})}(\rho_{A_1A_2}) &\simeq -\lim_{k\to 1}[\mathcal{A}_k^{(i)} + \log C_k] \\ &= -\lim_{k\to 1}\left[\beta E_{\partial R}\left(\frac{k}{2}-1\right) + \beta_t T\frac{k}{2} + \log C_k\right] \\ &= \frac{1}{2}(\beta E_{\partial R} - \beta_t T) + \log\frac{8}{3\pi}, \end{aligned} \quad (70)$$

with the Catalan numbers C_k and $C_1 = \frac{8}{3\pi}$ here taking into account the degeneracy in the choice of the geodesic coloring τ for the bulk.

We have then a transition from an unentangled phase to an area law behavior, as expected by the topological character of the entanglement contributions. In fact, it is possible to write $E_N^{(\text{island})}(\rho_{A_1A_2})$ as a generalization of the Ryu-Takayanagi formula for entanglement entropy [69]. By defining the minimal surfaces that separate the entanglement wedges relative to each subsystem as $|\gamma_{A_1}|$, $|\gamma_{A_2}|$, and $|\gamma_B|$, it is straightforward to see that

$$|\gamma_{A_1}| = E_{A_1}, \qquad |\gamma_{A_2}| = E_{A_2}, \qquad |\gamma_B| = T \quad (71)$$

where E_{A_1}, E_{A_2} are the number of edges in A_1 and A_2 respectively.

Hence, since $E_{A_1} + E_{A_2} = E_{\partial R}$ we can write Eq. (70) as

$$E_N^{(\text{island})}(\rho_{A_1A_2}) = \frac{1}{2}[\beta(|\gamma_{A_1}| + |\gamma_{A_2}|) - \beta_t|\gamma_B|] + \log\frac{8}{3\pi}. \quad (72)$$

This is a generalization of the Ryu-Takayanagi formula found in [61] to the case of nonhomogeneous mixed spin-network states (two temperatures). As for the previous works, it can be expressed as *mutual information* between the subsystem A_1 and A_2:

$$\begin{aligned} E_N^{(\text{island})} &= \frac{1}{2}[S(\rho_{A_1}) + S(\rho_{A_2}) - S(\rho_{A_1A_2})] + \log\frac{8}{3\pi} \\ &= \frac{1}{2}I(A_1 : A_2) + \log\frac{8}{3\pi}. \end{aligned} \quad (73)$$

In the island regime, then, the logarithmic negativity is *always* nonzero, and scales with the total area of the boundary of R, namely $\beta E_{\partial R}$, minus a negative correction

[8]The configurations in which on all the vertices in R there is X or X^{-1} belong to this regime too. In these two extreme cases the domain wall S is expelled from the bulk, and invades some of the boundary, in particular the region corresponding to the Hilbert space with minimal dimension among $\mathcal{H}_{A_1}$ and $\mathcal{H}_{A_2}$, which in turn is equivalent to considering the minimal area between the areas of the regions A_1 and A_2.

that depends linearly on the number of tags. This implies that the boundary state is necessarily entangled. In particular, the presence of the environment reflects a saturation of the entanglement of the two boundary subsystems. The logarithmic negativity only depends on the size of the system and of the environment, but it is independent of the specific bipartition of the boundary.

Finally, in the bipartite regime, the action with minimal energy is given by

$$\mathcal{A}_k^{(X)} = \beta S(k-2) + \beta_t T(k-1), \tag{74}$$

and the typical logarithmic negativity reads as

$$\begin{aligned} E_N^{(\text{bipartite})}(\rho_{A_1A_2}) &\simeq -\lim_{k\to 1}\mathcal{A}_k^{(X)} \\ &= -\lim_{k\to 1}[\beta S(k-2) + \beta_t T(k-1)] \\ &= \beta S. \end{aligned} \tag{75}$$

In this regime, negativity scales with the area of the internal domain wall S. In particular, we see from (75) that in this regime we could achieve a PPT state for the boundary only by setting S to 0, where a PPT state would correspond to a disconnected graph as expected.

Such a behavior is consistent with a limit toward a bipartite *pure* boundary state setting corresponding to vanishing tags (trivial topology) [63].

Altogether, the effective topology of the bounded region is reflected in the multipartite entanglement of its *tagged* spin-networks state description. Beside the toy model example, the proposed analysis can be easily generalized for graphs with a generic number of vertices, with more than one open edge attached to each boundary vertex, and with clusters of tags restricted to a subregion of the bulk graph. The universal character of the result is indeed associated to the typical behavior of the randomized system in the large spin regime.

VIII. DISCUSSION

In the framework of loop quantum gravity, quantum geometry states corresponding to *bounded* regions of $3D$ space with *uniform curvature* can be described via superpositions of *tagged* spin networks with boundary. Curvature naturally builds up at the spin-network vertices in the form of topological defects described by spin tags, as the result of the *partial tracing* over nontrivial $SU(2)$ holonomies of the Ashtekar connection along the network.

In the presence of a boundary, a quantum geometry wave function generally behaves as a map encoding the bulk information into the boundary Hilbert space. In the proposed analysis, we generalize such a bulk-to-boundary mapping as to include the space of bulk topological defects, effectively described as extra (inner) boundary degrees of freedom.[9] In the resulting *extended boundary* state, bulk information is *shared* among generically entangled boundary spins and tags: the surface and the intrinsic curvature of the quantum space region are entangled. Remarkably, the degree of quantum correlations among boundary subregions is affected by the presence of the bulk curvature, which plays the role of a hidden environment for the mixed outer boundary state.

The effect of the curvature on the boundary entanglement is the focus of our analysis. We model the generalized boundary mapping on a tripartite (A_1, A_2, B) system and consider the reduced boundary state $\rho_{A_1A_2}$ obtained via a trace over the space of tags (system B). We further characterize the coarse viewpoint of a boundary observer by considering a *random measurement* on the bulk state, thereby ultimately dealing with a *random mixed state* for the boundary.

The entanglement of the bipartite mixed boundary is quantified via a measure of logarithmic negativity, along the lines of the recent results in [61,69,72]. Concretely, we restrict the analysis to a class of states characterized by graphs colored by the same spin j on each edge and dressed with a tag of corresponding recoupled spin J at each vertex. We call this setting a *cluster of tags*. The full computation is carried on for a simple cluster of four tags given in Sec. VII A. By using standard replica techniques for random tensor network, this computation is ultimately mapped to the evaluation of the minimal action of a classical generalized Ising-like statistical model on the spin-network graph, in the limit of vanishing temperature (see [61] and references therein).

As a first general result, we find that the Ising-like model action dual to the random spin network generally splits into two main contributions:

$$A_1^{(k)} = A_{\text{topology}}^{(k)} + A_{\text{phys}}^{(k)} \tag{76}$$

that is a contribution $A_{\text{topology}}^{(k)}$ which accounts for the entanglement induced by the *topology* of the spin network graph and a second one, $A_{\text{phys}}^{(k)}$, encoding the bulk intertwiner entanglement. The former, in particular, further splits into two very distinct contributions,

$$A_{\text{topology}}^{(k)} = A_{\text{edges}}^{(k)} + A_{\text{tags}}^{(k)},$$

respectively associated to the *connectivity* of the bulk network (trivial topology), induced by maximally entangled edge states, and to the presence of the tags. The last term is therefore specific to the case of spin-network states with topological defects.

[9] In fact, we can think of bulk tags as the recoupled dangling bulk spins dual to the surface of holes cut out of a planar spin-network graph.

In a topologically trivial setting, as shown in [61], the first term in (76) is associated to an area law scaling of the entanglement of the boundary, while bulk intertwiners' entanglement can be interpreted in analogy with [67]. We leave the characterization of the random bulk contribution for future work, while focusing on the nontrivial topological contribution to the action.

Within the typical regime, the entanglement phases of the random boundary state can be described solely in terms of the relative dimensions of the three subsystems A_1, A_2, and B,[10] via the parameter

$$q = \beta_t T/\beta E_{\partial R} = \frac{\log[\dim(B)]}{\log[\dim(A_1)\dim(A_2)]}, \tag{77}$$

which expresses the ratio of bulk curvature over the boundary surface, with $E_{\partial R} = E_{A_1} + E_{A_2}$. Two main entanglement phases are separated by a critical point at $q = 1$.

For $1 - 2S/E_{\partial R} < q < 1$, the curvature environment mediates the entanglement of the boundary. The logarithmic negativity, modulo degeneracy, scales with the area of the cluster boundary with a negative correction which depends linearly on the number of tags. We have

$$\begin{aligned} E_N^{(\text{island})}(\rho_{A_1A_2}) &\propto \frac{1}{2}\beta E_{\partial R}(1-q) \\ &= \frac{1}{2}[\beta(|\gamma_{A_1}| + |\gamma_{A_2}|) - \beta_t|\gamma_B|] \end{aligned} \tag{78}$$

with $|\gamma_{A_1}| = E_{A_1}$,$|\gamma_{A_2}| = E_{A_2}$, and $|\gamma_B| = T$, the minimal surfaces separating the entanglement wedges relative to each subsystem. This is a generalization of the Ryu-Takayanagi formula for entanglement entropy for the tripartite setting, in agreement with [61,69], and it can be expressed as *mutual information* between the subsystem A_1 and A_2.

Finally, for $q < 1–2S/E_{\partial R}$, when the curvature environment is much smaller than the boundary system, we tend to a bipartite setting, and the typical logarithmic negativity scales with the area of the surface S separating A_1 and A_2 through the boundary. In this case, we find

$$E_N^{(\text{bipartite})}(\rho_{A_1A_2}) \propto \beta S. \tag{79}$$

Notice that the value of S cannot be tuned in our analysis, as the surface is fixed by the spin-network connectivity for the given graph. However, assuming some regularity of the graph, one can geometrically relate this value to the bipartition of the boundary. For instance, assuming a generic tagged graph with a large density of vertices, dual to a three ball, we can imagine the minimal surface S to be approximated by the intersection of the sphere and a generic plane, which divides A_1 from A_2 on the boundary of R. In this case, we can approximately set

$$S \approx j^2 \frac{E_{A_1}E_{A_2}}{E_{\partial R}}. \tag{80}$$

Therefore, we see that the island condition is favored when the dimension of the two subsystems A_1 and A_2 is well balanced, since S is maximized by high values of both E_{A_1} and $E_{A_2} = E_{\partial R} - E_{A_1}$. Conversely, from the condition $q < 1–2S/E_{\partial R}$, the bipartite regime is favored when the two boundary subregions A_1 and A_2 are extremely asymmetric in extension (smaller S).

In particular, we can describe the transition from the island to the bipartite regime by using (80) in the condition $\mathcal{A}_k^{(\text{bipartite})} < \mathcal{A}_k^{(\text{island})}$. We find

$$\left(\frac{E_{A_1}}{E_{\partial R}}\right)^2 - \frac{E_{A_1}}{E_{\partial R}} + (1-q) > 0. \tag{81}$$

Therefore, for $0 < q < 1$, we can identify two critical points between the island and the bipartition phases,

$$c_{1,2}^*(q) = \frac{1}{2} \pm \frac{1}{2}\sqrt{q}. \tag{82}$$

The behavior of the negativity is well described by the generalized Page curve in Fig. 10. As a general feature of a tripartite random state, we find that the degree of correlation of the two boundary subregions A_1, A_2 depends on the degree of quantum correlations the two boundary systems have with the curvature environment. By varying the

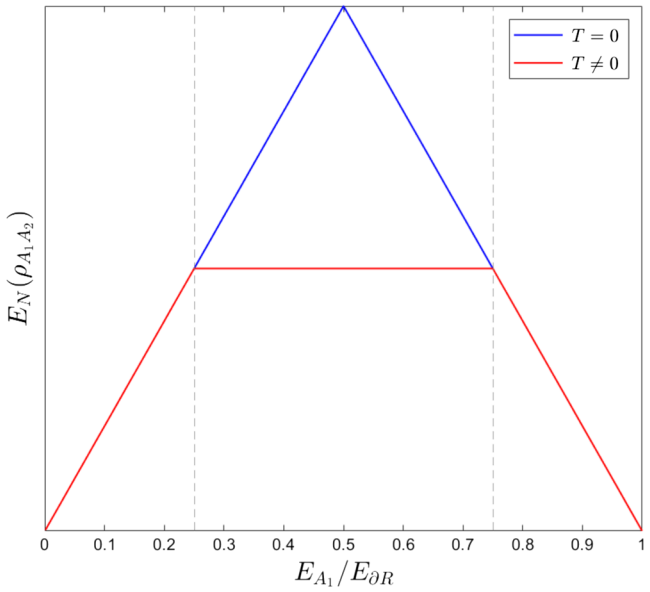

FIG. 10. In red the generalized Page curve of the logarithmic negativity for the random mixed state $\rho_{A_1A_2}$. In red, how the Page curve would appear for random pure states.

[10]Where $\dim(A_1) = (d_j)^{E_{A_1}}$, $\dim(A_2) = (d_j)^{E_{A_2}}$, and $\dim(B) = (d_j)^T$ respectively.

relative size of the two subsystems, the logarithmic negativity shows an initial increase and a final decrease in analogy with the Page curve. When $T = 0$ (trivial topology), $c_1^*(0) = c_2^*(0) = 1/2$, and we get back the standard Page curve [91] (no tripartition). As soon as $T \neq 0$, we enter in the intermediate island regime, and the negativity has a plateau. In this regime the logarithmic negativity only depends on the size of the system and of the environment but not on how the system is partitioned.

On the other hand, for $q > 1$, corresponding to a large tags environment with respect to the boundary system, the logarithmic negativity vanishes. The boundary system is almost fully entangled with the environment with little quantum correlation between A_1 and A_2. In particular, the area law behavior is lost. This suggests that large curvature is associated to a *maximally* mixed boundary state $\rho_{A_1A_2}$. Such a thermal character of the boundary state as an effect of curvature is in strong analogy to the quantum gravity formulation of the hoop conjecture proposed in [90], where again the typicality of the random state, in the large spin regime, plays a crucial role. It is worth remarking that the entanglement phases in our model have a purely *kinematical* characterization, as for given generalized Ising boundary conditions both spin values and graph connectivity are fixed. Still, we can imagine a dynamic change of relative dimensions of the extended boundary subregions as a natural effect of the graph changing loop quantum gravity dynamics. A dynamical characterization of an analog tripartite setting, with a direct interpretation of the Page curve in terms of entanglement transitions was recently proposed in [70,92] to describe an evaporating black hole in AdS/CFT.

If we consider that the large spin regime we have been working in is necessarily associated with a semiclassical limit for our quantum geometry states, then we can tentatively interpret the formulas found for the entanglement negativity in terms of areas of a bounded $3D$ region of a Riemannian manifold and look for a direct relation with its Ricci curvature. Indeed, we know that the value of the scalar curvature $\mathcal{R}$ of a Riemannian n-manifold $\mathcal{M}$ at a point p can be quantified by the ratio of the area of the $(n-1)$-dimensional boundary of a ball of radius ε in $\mathcal{M}$ to that of a corresponding ball in the Euclidean space. For small ε, the ratio is given by [93,94]

$$\frac{\mathrm{Area}(\partial B_\varepsilon(p) \subset \mathcal{M})}{\mathrm{Area}(\partial B_\varepsilon(0) \subset \mathbb{R}^n)} = 1 - \frac{\mathcal{R}}{6n}\varepsilon^2 + O(\varepsilon^3). \tag{83}$$

Now, in the semiclassical limit, for $n = 3$, we can easily associate the area of the boundary of a flat three-ball region with the sum of the areas of the triangles dual to the open edge spins comprising the boundary of R (no tags), that is $\mathrm{Area}(\partial B_\varepsilon(0)) \simeq \beta E_{\partial R}(\varepsilon)$, where $E_{\partial R}(\varepsilon)$ counts the number of boundary edges at a certain scale ε, that could be considered as the chosen coarse-graining scale of our theory. In case of the curved three ball in $\mathcal{M}$, however, we expect this value to be modified by the presence of tags. In particular, if we assume for simplicity

$$\mathrm{Area}(\partial B_\epsilon(p)) \simeq \beta E_{\partial R}(\epsilon) + \kappa\beta_t T(\epsilon) \tag{84}$$

namely a correction linear in the number of tags (positive or negative depending on the sign of the proportionality constant κ), where $T(\epsilon)$ indicates the number of tags within a given coarsegraining scale ϵ. Under this assumption, the ratio in (83) gives us a direct relation between the entanglement phase parameter and the Ricci curvature:

$$q(\varepsilon) \simeq -\frac{\mathcal{R}}{18\kappa}\varepsilon^2. \tag{85}$$

For instance, in this light, we find a nice relation between the area scaling negativity (or mutual information) in (78) and the geometric relation in (83). Such a relation is consistent with the interpretation of our results and hints toward a characterization of the curvature in purely information theoretic terms [95].

Let us then conclude with a few further remarks. A first remark is concerning the nongauge invariant character of the degrees of freedom considered in our analysis. A spin network's tags are not different from boundary dangling spins, whose presence indeed breaks gauge invariance at the boundary. The entanglement we describe among boundary spins and tags cannot be measured in terms of gauge invariant observables; hence it is considered as nonphysical in loop quantum gravity [96]. Nevertheless, we expect such a topological layer of entanglement to become essential in modeling the emergence of spacetime connectivity as soon as we allow both edge and tag spins to be physical at some higher energy scale, where we expect gauge invariance to break. This perspective would require an extension of the kinematical description of quantum geometry in loop quantum gravity, which is in part provided by the second quantized formalism of group field theory [20]. Differently, one can take the present analysis as a toy model for an ultimate description of the entanglement structure of *edge modes'* degrees of freedom at the interface of subsystems [97–99]. In this sense, we expect the described universal features of the interface entanglement in the large spin regime to be general.

A final remark has to do with the interplay of intrinsic and extrinsic geometry in loop quantum gravity. As shown in [86,100], in loop quantum geometry states, nontrivial Ashtekar-Barbero holonomies can be thought of alternatively as intrinsic or *extrinsic curvature*. In particular, it is possible to compensate the tag (closure defect) induced by the coarse-graining by the action of a Lorentz boost. Actually, this amounts to replacing the tag recoupling the edge spins at the vertex with an extra virtual edge carrying an $SL(2,\mathbb{C})$ holonomy. The result is a intrinsically flat quantum 3D geometry with a non-flat local embedding

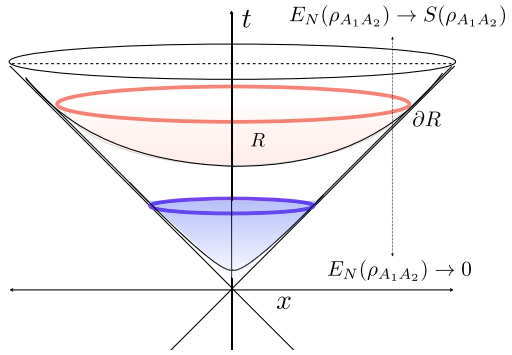

FIG. 11. Milne-like [103] spacetime sliced by $3D$ surfaces with hyperbolic embedding. Close to Milne's big bang, the quantum realization of such surfaces has vanishing negativity, $E_N(\rho_{A_1A_2}) \to 0$. As time increases, the negativity of the $2D$ cosmological horizon grows and tends toward bipartite entanglement entropy, $E_N(\rho_{A_1A_2}) \to S(\rho_{A_1A_2})$ at large times.

in 4D spacetime. This suggests a natural relation between embedding and entanglement to which we shall dedicate further investigation in future work. For instance, one could figure the phase transition previously described, between a maximally entangled ($q \ll 1$) to a maximally mixed ($q \gg 1$) boundary state, as being described by a sequence of quantum $3D$ spacelike slices with a gradient in curvature (see Fig. 11). If we embed such slices, via boost, in the hyperbolic space, we would get a transition from almost flat bounded regions with a large corner surface corresponding to a maximally entangled boundary state to highly curved regions with a small corner surface corresponding to maximally mixed boundary state. A similar setting then recalls the conjectured behavior of spacetime geometry while approaching the cosmological singularity [see, e.g., the Belinski–Khalatnikov–Lifshitz (BKL) conjecture [101]]. A quantitative analysis of a similar scenario could be directly investigated within a nonperturbative quantum gravity setting by looking at a *multipartite* quantum $3D$ space geometry as the boundary of a spin-foam quantum spacetime bulk [19] (see also [102] for a different approach to the BKL conjecture in loop quantum cosmology). We leave this analysis for future work.

ACKNOWLEDGMENTS

The authors would like to thank A. Hamma and D. Oriti for useful discussions on the preliminary results of the work, M. Arzano for suggesting the relation between a set of boost embedded quantum 3D space regions and Milne geometry, and H. Haggard for remarking upon a possible use of the proposed multipartite setting toward a description of the BKL conjecture in quantum gravity.

[1] M. Van Raamsdonk, Gen. Relativ. Gravit. **42**, 2323 (2010).
[2] B. Swingle, Phys. Rev. D **86**, 065007 (2012).
[3] E. Bianchi and R. C. Myers, Classical Quantum Gravity **31**, 214002 (2014).
[4] N. Lashkari, M. B. McDermott, and M. Van Raamsdonk, J. High Energy Phys. 04 (2014) 195.
[5] T. Faulkner, M. Guica, T. Hartman, R. C. Myers, and M. Van Raamsdonk, J. High Energy Phys. 03 (2014) 051.
[6] T. Jacobson, Phys. Rev. Lett. **116**, 201101 (2016).
[7] C. Cao, S. M. Carroll, and S. Michalakis, Phys. Rev. D **95**, 024031 (2017).
[8] B. Swingle and M. Van Raamsdonk, arXiv:1405.2933.
[9] X.-L. Qi, arXiv:1309.6282.
[10] J. M. Maldacena, Int. J. Theor. Phys. **38**, 1113 (1999).
[11] B. Swingle, arXiv:1209.3304.
[12] A. Bhattacharyya, Z.-S. Gao, L.-Y. Hung, and S.-N. Liu, J. High Energy Phys. 08 (2016) 086.
[13] N. Bao, C. Cao, S. M. Carroll, A. Chatwin-Davies, N. Hunter-Jones, J. Pollack, and G. N. Remmen, Phys. Rev. D **91**, 125036 (2015).
[14] N. Bao, G. Penington, J. Sorce, and A. C. Wall, J. High Energy Phys. 11 (2019) 069.
[15] Z. Yang, P. Hayden, and X.-L. Qi, J. High Energy Phys. 01 (2016) 175.
[16] C. Rovelli, Living Rev. Relativity **11**, 5 (2008).
[17] T. Thiemann, *Modern Canonical Quantum General Relativity*, Cambridge Monographs on Mathematical Physics (Cambridge University Press, Cambridge, England, 2007).
[18] C. Rovelli and F. Vidotto, *Covariant Loop Quantum Gravity: An Elementary Introduction to Quantum Gravity and Spinfoam Theory* (Cambridge University Press, Cambridge, England, 2014).
[19] A. Perez, Living Rev. Relativity **16**, 3 (2013).
[20] D. Oriti, Classical Quantum Gravity **33**, 085005 (2016).
[21] R. Penrose, Angular momentum: An approach to combinatorial spacetime, in *Quantum Theory and Beyond*, edited by T. Bastin (Cambridge University Press, Cambridge, England, 1971), pp. 151–180.
[22] R. Penrose and W. Rindler, *Spinors and Space-Time*, Cambridge Monographs on Mathematical Physics Vol. 1 (Cambridge University Press, Cambridge, England, 1984).
[23] C. Rovelli and L. Smolin, Phys. Rev. D **52**, 5743 (1995).
[24] A. Ashtekar, Phys. Rev. Lett. **57**, 2244 (1986).
[25] A. Ashtekar, M. Reuter, and C. Rovelli, *From General Relativity to Quantum Gravity* (Cambridge University Press, Cambridge, 2015).
[26] A. Ashtekar and E. Bianchi, Rep. Prog. Phys. **84**, 042001 (2021).

[27] E. Bianchi and R. C. Myers, Classical Quantum Gravity **31**, 214002 (2014).
[28] W. Donnelly, Phys. Rev. D **77**, 104006 (2008).
[29] W. Donnelly, Phys. Rev. D **85**, 085004 (2012).
[30] B. Baytaş, E. Bianchi, and N. Yokomizo, Phys. Rev. D **98**, 026001 (2018).
[31] E. R. Livine, Phys. Rev. D **97**, 026009 (2018).
[32] C. Delcamp, B. Dittrich, and A. Riello, J. High Energy Phys. 11 (2016) 102.
[33] E. Bianchi, J. Guglielmon, L. Hackl, and N. Yokomizo, Phys. Rev. D **94**, 086009 (2016).
[34] E. Bianchi, L. Hackl, and N. Yokomizo, Phys. Rev. D **92**, 085045 (2015).
[35] G. Chirco, D. Oriti, and M. Zhang, Phys. Rev. D **97**, 126002 (2018).
[36] G. Chirco, I. Kotecha, and D. Oriti, arXiv:1811.00532.
[37] G. Chirco, I. Kotecha, and D. Oriti, Phys. Rev. D **99**, 086011 (2019).
[38] D. Oriti, arXiv:1807.04875.
[39] G. Chirco, H. M. Haggard, A. Riello, and C. Rovelli, Phys. Rev. D **90**, 044044 (2014).
[40] G. Chirco, C. Rovelli, and P. Ruggiero, Classical Quantum Gravity **32**, 035011 (2015).
[41] A. Hamma, L.-Y. Hung, A. Marciano, and M. Zhang, Phys. Rev. D **97**, 064040 (2018).
[42] E. Bianchi and A. Satz, Phys. Rev. D **99**, 085001 (2019).
[43] S. Raju, Int. J. Mod. Phys. D **28**, 1944011 (2019).
[44] B. Dittrich, C. Goeller, E. Livine, and A. Riello, Nucl. Phys. **B938**, 807 (2019).
[45] B. Dittrich, C. Goeller, E. R. Livine, and A. Riello, Classical Quantum Gravity **35**, 13LT01 (2018).
[46] E. R. Livine and D. R. Terno, arXiv:gr-qc/0603008.
[47] F. Girelli and E. R. Livine, Classical Quantum Gravity **22**, 3295 (2005).
[48] E. Bianchi, J. Guglielmon, L. Hackl, and N. Yokomizo, Phys. Rev. D **94**, 086009 (2016).
[49] A. Feller and E. R. Livine, Classical Quantum Gravity **35**, 045009 (2018).
[50] F. Anzà and G. Chirco, Phys. Rev. D **94**, 084047 (2016).
[51] P. A. Höhn, J. Phys. Conf. Ser. **880**, 012014 (2017).
[52] G. Chirco, F. M. Mele, D. Oriti, and P. Vitale, Phys. Rev. D **97**, 046015 (2018).
[53] E. Bianchi and E. R. Livine, arXiv:2302.05922.
[54] H. Sahlmann and W. Sherif, arXiv:2302.03612.
[55] H. M. Haggard, J. Lewandowski, and H. Sahlmann, arXiv:2302.02840.
[56] L. Marchetti, D. Oriti, A. G. A. Pithis, and J. Thürigen, Phys. Rev. Lett. **130**, 141501 (2023).
[57] G. Czelusta and J. Mielczarek, Phys. Rev. D **103**, 046001 (2021).
[58] L. Freidel, M. Geiller, and W. Wieland, arXiv:2302.12799.
[59] Q. Chen and E. R. Livine, Classical Quantum Gravity **38**, 155019 (2021).
[60] Q. Chen and E. R. Livine, Classical Quantum Gravity **39**, 215013 (2022).
[61] S. Cepollaro, G. Chirco, G. Cuffaro, and V. D'Esposito, Phys. Rev. D **107**, 086003 (2023).
[62] G. Chirco, A. Goeßmann, D. Oriti, and M. Zhang, Classical Quantum Gravity **37**, 095011 (2020).
[63] G. Chirco, E. Colafranceschi, and D. Oriti, Phys. Rev. D **105**, 046018 (2022).
[64] E. Colafranceschi, G. Chirco, and D. Oriti, Phys. Rev. D **105**, 066005 (2022).
[65] E. Colafranceschi, S. Langenscheidt, and D. Oriti, arXiv:2207.07625.
[66] E. Colafranceschi and G. Adesso, AVS Quantum Sci. **4**, 025901 (2022).
[67] P. Hayden, S. Nezami, X.-L. Qi, N. Thomas, M. Walter, and Z. Yang, J. High Energy Phys. 11 (2016) 009.
[68] X.-L. Qi, Z. Yang, and Y.-Z. You, J. High Energy Phys. 08 (2017) 060.
[69] X. Dong, X.-L. Qi, and M. Walter, J. High Energy Phys. 06 (2021) 024.
[70] J. Kudler-Flam, V. Narovlansky, and S. Ryu, J. High Energy Phys. 02 (2022) 076.
[71] J. Kudler-Flam, V. Narovlansky, and S. Ryu, PRX Quantum **2**, 040340 (2021).
[72] H. Shapourian, S. Liu, J. Kudler-Flam, and A. Vishwanath, PRX Quantum **2**, 030347 (2021).
[73] E. R. Livine, Classical Quantum Gravity **31**, 075004 (2014).
[74] C. Charles and E. R. Livine, Gen. Relativ. Gravit. **48**, 1 (2016).
[75] M. B. Hastings, I. González, A. B. Kallin, and R. G. Melko, Phys. Rev. Lett. **104**, 157201 (2010).
[76] A. Peres, Phys. Rev. Lett. **77**, 1413 (1996).
[77] M. B. Plenio, Phys. Rev. Lett. **95**, 090503 (2005).
[78] K. Życzkowski, P. Horodecki, A. Sanpera, and M. Lewenstein, Phys. Rev. A **58**, 883 (1998).
[79] K. Życzkowski, Phys. Rev. A **60**, 3496 (1999).
[80] J. Eisert and M. B. Plenio, J. Mod. Opt. **46**, 145 (1999).
[81] G. Vidal and R. F. Werner, Phys. Rev. A **65**, 032314 (2002).
[82] P. Ruggiero, V. Alba, and P. Calabrese, Phys. Rev. B **94**, 035152 (2016).
[83] C. Rovelli and F. Vidotto, *Covariant Loop Quantum Gravity* (Cambridge University Press, Cambridge, England, 2014).
[84] E. Bianchi, P. Doná, and S. Speziale, Phys. Rev. D **83**, 044035 (2011).
[85] L. Freidel and S. Speziale, Phys. Rev. D **82**, 084040 (2010).
[86] E. R. Livine, Classical Quantum Gravity **36**, 185009 (2019).
[87] E. R. Livine, Europhys. Lett. **123**, 10001 (2018).
[88] E. Bianchi and P. Donà, Phys. Rev. D **100**, 105010 (2019).
[89] Q. Chen and E. R. Livine, Classical Quantum Gravity **38**, 155019 (2021).
[90] F. Anzà and G. Chirco, Phys. Rev. Lett. **119**, 231301 (2017).
[91] D. N. Page, Phys. Rev. Lett. **71**, 1291 (1993).
[92] G. Penington, S. H. Shenker, D. Stanford, and Z. Yang, J. High Energy Phys. 03 (2022) 205.
[93] S. Gallot, D. Hulin, and J. Lafontaine, *Riemannian Geometry*, Universitext (Springer, Berlin, Heidelberg, 2004).
[94] *Eigenvalues in Riemannian Geometry*, edited by I. Chavel, B. Randol, and J. Dodziuk, Pure and Applied Mathematics, Vol. 115 (Elsevier, New York, 1984), pp. 303–333.

[95] S. Cepollaro, G. Chirco, and G. Cuffaro (to be published).
[96] C. Rovelli, Found. Phys. **44**, 91 (2014).
[97] W. Donnelly, L. Freidel, S. F. Moosavian, and A. J. Speranza, J. High Energy Phys. 09 (2021) 008.
[98] L. Ciambelli, R. G. Leigh, and P.-C. Pai, Phys. Rev. Lett. **128**, 171302 (2022).
[99] V. Kabel and W. Wieland, Phys. Rev. D **106**, 064053 (2022).
[100] L. Freidel and E. R. Livine, Gen. Relativ. Gravit. **51**, 9 (2019).
[101] V. A. Belinskiĭ, E. M. Lifshitz, and I. M. Khalatnikov, Sov. Phys. Usp. **13**, 745 (1971).
[102] A. Ashtekar, A. Henderson, and D. Sloan, Phys. Rev. D **83**, 084024 (2011).
[103] V. Mukhanov, *Physical Foundations of Cosmology* (Cambridge University Press, Oxford, 2005).